

Latency-Controlled Neural Architecture Search for Streaming Speech Recognition

Liqiang He¹, Shulin Feng¹, Dan Su¹, Dong Yu²

¹Tencent AI Lab, Shenzhen, China

²Tencent AI Lab, Bellevue WA, USA

{andyliqhe, shulinfeng, dansu, dyu}@tencent.com

Abstract

Recently, neural architecture search (NAS) has attracted much attention and has been explored for automatic speech recognition (ASR). Our prior work has shown promising results compared with hand-designed neural networks. In this work, we focus on streaming ASR scenarios and propose the latency-controlled NAS for acoustic modeling. First, based on the vanilla neural architecture, normal cells are altered to be causal cells, in order to control the total latency of the neural network. Second, a revised operation space with a smaller receptive field is proposed to generate the final architecture with low latency. Extensive experiments show that: 1) Based on the proposed neural architecture, the neural networks with a medium latency of 550ms (millisecond) and a low latency of 190ms can be learned in the vanilla and revised operation space respectively. 2) For the low latency setting, the evaluation network can achieve more than 19% (average on the four test sets) relative improvements compared with the hybrid CLDNN baseline, on a 10k-hour large-scale dataset. Additional 11% relative improvements can be achieved if the latency of the neural network is relaxed to the medium latency setting.

Index Terms: neural architecture search, low latency, streaming/online speech recognition

1. Introduction

Performance improvement of automatic speech recognition (ASR) systems owes much to the dedicated hand-designed model architectures. However, designing state-of-the-art neural network architectures requires a lot of expert knowledge and takes ample time. Recently, there has been rapid progress in neural architecture search (NAS) research, which brought significant performance improvement in the computer vision field. There has been also many research work applying NAS into audio and speech processing tasks, such as acoustic scene classification [1], ASR [2, 3, 4], keyword spotting [5], speaker recognition [6] and text to speech (TTS) [7]. Among these, our prior work [3] explored NAS in the LVCSR task. We adopted the differentiable framework and revised the search space for the final architecture with low complexity. The experimental results demonstrate supreme performance on a 10k-hour dataset.

In many real scenarios, low latency streaming ASR (a.k.a., online ASR) is of critical importance. Since NAS has shown great potential in our ASR experiments, a problem naturally arising is how to perform latency-controlled NAS for streaming ASR. In speech processing tasks, the latency generally depends on two aspects: the computation overhead introduced by the model complexity, and the future information needed when processing current input. There have been many works considering model complexity in NAS to achieve better speed/accuracy

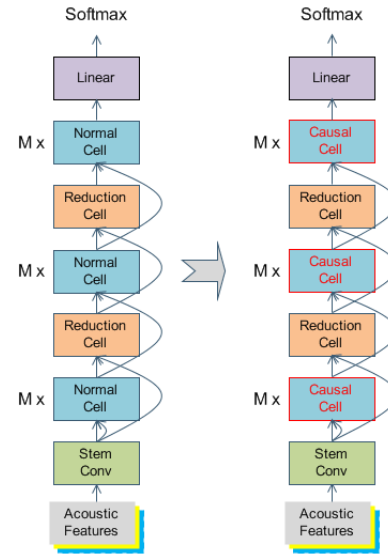


Figure 1: *The vanilla neural architecture [3] (left) without the context constraint, and the latency-controlled neural architecture (right) as proposed by our work.*

trade-off [8, 9, 10, 11]. Most of the works focus on reducing the computational overhead although limiting the lookahead frames is also essential to reduce the overall latency.

So far, there are two kinds of streaming ASR systems in industrial applications: the hybrid system and the end-to-end system. While end-to-end ASR systems have been proven to be competitive with the conventional hybrid systems, they often require to see more future contextual information, with a typical latency over 500ms, to achieve similar performance. In this work, we introduce latency constraints to the search space of NAS. We compared our latency-controlled NAS with a strong hybrid CLDNN-based system on a 10k-hour large-scale dataset. Experimental results show that the resulted evaluation network with a latency of 190ms reduced character error rate (CER) by more than 19% (averaged on the four test sets) relatively over the hybrid CLDNN baseline with a latency of 180ms. An additional 11% relative CER reduction can be achieved if we relax the latency to 550ms.

The contributions of this paper are as follows: 1) We propose a novel neural architecture with the normal cells replaced with the causal cells that do not depend on future context. 2) We present a revised operation space with a smaller receptive field with which low latency can be enforced in the final architecture. 3) We show that the searched architectures with the medium and low latency settings achieve significant perfor-

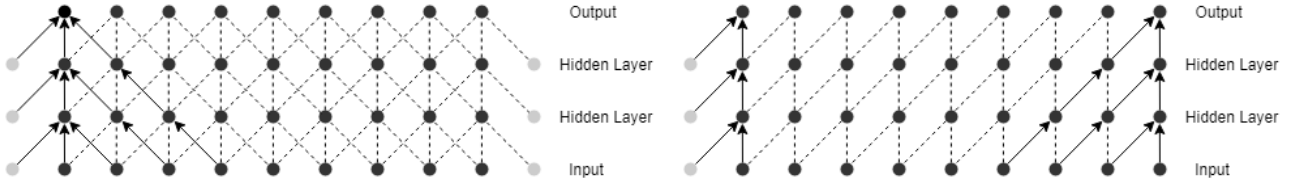


Figure 2: Visualization of a stack of operation layers: the vanilla operations (left) in the normal cell, and the causal operations (right) in the causal cell as proposed by our work. Gray dots are represented as the padding nodes.

mance improvements on the large-scale dataset, compared with the conventional hand-designed model.

2. Vanilla Neural Architecture Search

This section gives a brief overview of the NAS method in [3], which is the vanilla NAS without the latency constraint, as shown in the left half of Figure 1.

In the search phase, following [12], the normal cell and the reduction cell are searched as the building blocks of the final architecture. The bi-chain-styled macro architecture [13] are adopted, as used in [14]. The two reduction cells are located at the 1/3 and 2/3 depth of the neural architecture respectively. The micro architecture [13] of the cell is a directed acyclic graph consisting of multiple intermediate nodes. Each node is a feature map, and each directed edge is associated with the candidate operation. The input nodes are defined as the outputs of the previous two cells. The output of the cell is obtained by applying a concatenation operation to all the intermediate nodes. Based on DARTS[14], a revised search space proposed by [3] facilitates the search algorithm to explore the convolutional architectures with low complexity for ASR tasks. Furthermore, progressive differentiable architecture search [15] is applied to the search procedure to bridge the depth gap between the search and evaluation phases.

In the evaluation phase, the evaluation networks are constructed with the searched architecture. Following the scalable method [12], by changing the number of the normal cells, the evaluation networks can be built with the corresponding model parameters for different ASR applications while keeping the number of the reduction cells unchanged.

3. Latency-Controlled Algorithm

The latency-controlled neural architecture proposed by this work modifies the neural architecture [3] for streaming ASR, as illustrated in the right half of Figure 1.

Section 3.1 introduces the proposed neural architecture with the causal cells. The causal operations in the causal cell are described in section 3.2. Finally, the search spaces with the medium and low latency settings are presented in section 3.3.

3.1. Architecture Description

The macro architecture of our NAS [3] is shown in the left half of Figure 1. The following issues hinder this architecture to be applied in the streaming scenarios: 1) Both the normal and reduction cells are designed without the context constraint, and the receptive field grows with the number of the stacked cells. 2) Concerning the scalable method [12], the latency of the evaluation network changes with the number of the stacked cells required by ASR applications. The evaluation networks are generated with very high and uncertain latency, so it's almost

impossible to be applied in streaming ASR applications.

To solve the latency problems of the vanilla neural architecture, we propose a novel macro architecture with the normal cells replaced with the causal cells, as shown in the right half of Figure 1. Different from the normal cell, operations in the causal cell only depend on the left (history) context. After this modification, the latency of the proposed neural architecture only comes from the reduction cells. Once the structure of the reduction cell is learned, the latency of the evaluation networks is determined. Thus, we only need to control the latency of the reduction cells in the search phase for online streaming applications.

3.2. Causal Operations

The vanilla candidate operations [3] with the right (future) context dependency in the convolutional cell are as follows: [average pooling, max pooling, separable convolution, dilated separable convolution]. The receptive field, including the right context, grows linearly with the number of the stacked operation layers, as depicted in the left half of Figure 2.

Concerning the context constraint, the causal convolution is proposed by WaveNet [16], and a masked convolution, equivalent to the causal convolution, is realized in [17]. Considering all the candidate operations, we adopt the causal convolution [16] for the following operations: separable convolution, and dilated separable convolution. Furthermore, we extend this causal method to the remaining operations: average pooling, and max pooling. Through this, we make sure that all the modified operations, namely causal operations, in the search space do not depend on any of the right contexts, as shown in the right half of Figure 2. The causal cells composed of the causal operations thus depend on none of the right contexts.

3.3. Medium and Low Latency Search Spaces

The latency of the reduction cell is determined by the following aspects: 1) The micro architecture of the searched cell is a principal factor to influence the total latency. 2) The right context dependency of each finally selected operation is another important consideration. Theoretically, the total latency is computed by the summation of the latency of each selected operation in the deepest path of the searched reduction cell.

Concerning the first issue, a range of micro architectures with different latencies can be searched from the same search space with random initial seeds. Theoretically, we can run the architecture search many times and choose the micro architecture with low latency. However, we found empirically that micro architectures with good performance always have high latency.

As for the second issue, the search algorithm automatically searches for the optimal architectures with the corresponding latency based on the different operation spaces. The architec-

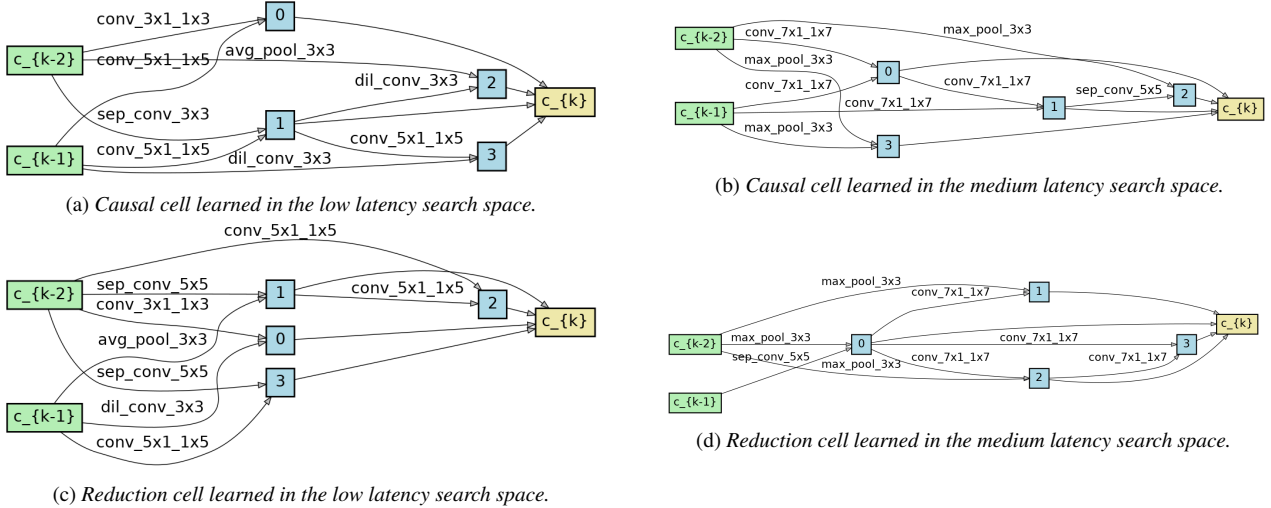


Figure 3: (a) and (c) are the cells (denoted as ASRNET-C with a latency of 190ms) learned in the low latency search space. (b) and (d) are the cells (denoted as ASRNET-D with a latency of 550ms) learned in the medium latency search space.

ture with low latency can be learned in the dedicated operation space. For comparison, the operation space in [3] is adopted for the medium latency search space, which is shared in both the causal and reduction cells. All the candidate operations in the causal cell are with the context constraint as stated in section 3.2. The optimal architecture for the medium latency setting is searched in the cited search space, as shown in the right half of Figure 3.

For the low latency search space, we propose the candidate set of the revised operation space as following: *[zero, 3x3 max pooling, 3x3 average pooling, 3x3 separable convolution, 5x5 separable convolution, 3x3 dilated separable convolution, 3x1 then 1x3 convolution, 5x1 then 1x5 convolution]*. Compared with the operation space in [3], the operations *[5x5 dilated separable convolution, 7x1 then 1x7 convolution]* are replaced with the operations *[3x1 then 1x3 convolution, 5x1 then 1x5 convolution]* for the smaller receptive fields. Furthermore, sequential modules with a *ReLU-Conv-BN* order are applied only once to the *separable convolution* in the revised operation space, while they are stacked twice in [3], leading to the double receptive field. As shown in the left half of Figure 3, the optimal architecture for the low latency setting is searched in the revised search space.

It should be noted that we use algorithmic latency induced by the right context dependency. Other factors, such as the computation delay of the neural network, are not taken into account. The procedures of the medium and low latency computations are described in section 4.5.

4. Experiments

4.1. Datasets

AISHELL-1 [18] is used as the small proxy dataset in the search phase. To verify the transferability of the searched architecture, two larger corpora are used in the evaluation phase: 1) AISHELL-2 [19] dataset, which contains 1000 hours of speech data from 1991 speakers, is used as the medium-scale dataset. 2) A 10k-hour multi-domain dataset [20] is used as the large-scale dataset. Further, AISEHLL-1 and AISEHLL-2 are augmented with 2-fold speed perturbation [21] in the experiments. To make the performance evaluation more comprehensive, re-

sults are reported on three types of test sets, which consist of hand-transcribed anonymized utterances extracted from reading speech (1001 utterances), conversation speech (1538 utterances), and spontaneous speech (2952 utterances). The above test sets are referred to as Read, Chat, and Spon respectively for short. Additionally, the AISHELL-2 development set (2500 utterances, short for DEV), recorded by high fidelity microphone, is used as the test set to provide a public benchmark.

4.2. Training setup

For acoustic features, we use 40-dimensional filterbanks extracted with a 25ms window with a stride of 10ms, extended with temporal first- and second-order differences. The length of the training utterances is filtered by a maximum limit of 1024 frames, and 4-frames-aligned padding was made for the length of each utterance to be fit for the two reduction layers. The CTC (connectionist temporal classification) learning framework is applied in the experiments, and the models are trained with multiple GPUs with BMUF [22]. We use the CI-syllable-based model units: 1394 Mandarin syllables, 39 English phones, and a blank. A beam search algorithm, using weighted finite-state transducers (WFSTs), performs the first-pass decoding with a pruned 5-gram language model and a second-pass rescoring with RNN model. The performance results are measured by Character Error Rate (CER).

4.3. Architecture Search

Refer to [3] for most of the hyperparameters and configurations of the search phase. We randomly split the training set of the AISHELL-1 dataset into two equal subsets, one half for learning network parameters and the other half for tuning the architecture parameters. We divide the search process into three stages [15]. In each stage, only network parameters are updated in the first 6 epochs, and both architecture and network parameters are alternately trained in the remaining 9 epochs. Following the search space regularization [15], the dropout probabilities are applied on the candidate operations *[dilated separable convolution, average pooling]*. Three sets of the dropout [0.00, 0.00, 0.00], [0.00, 0.05, 0.10], [0.00, 0.10, 0.20] are used, and the values in each set correspond to three stages, respectively. Besides, the discovered causal cells are restricted to keep at most

Table 1: *Token accuracies (Acc) and evaluation costs (Cost) of the networks on the AISHELL-1 dataset. Abbreviations: L is the number of cells, and C is the initial number of channels.*

Small	Params (M)	Acc (%)	Cost (hours)
ASRNET-C (L=17,C=25)	6.4	90.93	13.6
ASRNET-D (L=17,C=22)	6.5	91.27	12.4

Table 2: *Comparison with medium-sized CLDNN on the AISHELL-2 dataset. Rel Imp refers to Relative Improvement.*

Medium	Params (M)	CER (%)	Rel Imp (%)
CLDNN (90ms)	37.0	8.59	/
CLDNN (180ms)	37.0	7.45	-
ASRNET-C (L=26,C=30)	11.1	6.28	15.70
ASRNET-C (L=26,C=34)	13.7	5.51	26.04
ASRNET-D (L=26,C=30)	14.4	5.71	23.36

2 average pooling. To alleviate the influence of randomness, the search process is repeated 3 times with different seeds for each dropout probability setting. Two optimal architectures are searched as follows: *ASRNET-C* with a low latency of 190ms as shown in the left half of Figure 3, and *ASRNET-D* with a medium latency of 550ms as depicted in the right half of Figure 3. The search process takes around 96 hours on 8 Tesla P40 GPUs.

4.4. Architecture Evaluation

On the AISHELL-1 dataset, the small evaluation networks contain 17 cells with initial channels of 25 and 22 for *ASRNET-C* and *ASRNET-D* respectively. The reason for different configurations is to make the model parameters of the two networks similar and ensure the fairness of comparison. Both networks are trained from scratch for 20 epochs with batch size 4 and the token accuracies are measured on the test set. As shown in Table 1, the performance of *ASRNET-D* with higher latency is slightly better than *ASRNET-C*. The training tasks are performed on 8 Tesla P40 GPUs. The widely used hybrid model CLDNN [23, 24] is used as the baseline. For the very low latency setting, CLDNN starts with two convolution layers with the kernel size 5×5 , and each layer is followed by the *max pooling* layer with the kernel size 2×1 and a stride of 2×1 . For the low latency setting, only the kernel size of the convolution layer is changed to 11×5 . The first value of the kernel is applied to the time axis and the second one to the frequency axis. Two settings are configured as follows: very low latency of 90ms, and low latency of 180ms.

On the AISHELL-2 dataset, the medium-sized evaluation networks contain 26 cells with initial channels of 30/34 and 30 for *ASRNET-C* and *ASRNET-D* respectively. The networks are trained from scratch for 15 epochs with batch size 4. The medium-sized CLDNN consists of 7 LSTM layers with 1024 nodes in each layer. As seen in Table 2, *ASRNET-C* with initial channels of 30 has achieved more than 15% relative improvements compared with the CLDNN baseline for the low latency setting. Based on the same initial configurations, the performance of the network *ASRNET-D* is better than the network *ASRNET-C*. However, based on similar model parameters, *ASRNET-C* with initial channels of 34 performs better than *ASRNET-D*. The training processes are accelerated by us-

Table 3: *Comparison with large-sized CLDNN on a 10k-hour dataset. CERs are measured on the four test sets.*

Large	Params (M)	Read (%)	Chat (%)	Spon (%)	DEV (%)
CLDNN (90ms)	55.12	3.35	32.52	31.75	6.31
CLDNN (180ms)	55.15	2.95	28.78	30.87	5.73
ASRNET-C (L=26,C=56)	32.8	2.22	25.45	24.26	4.54
ASRNET-D (L=26,C=50)	35.8	1.74	22.52	22.95	4.27

ing 24 Tesla P40 GPUs.

On a 10k-hour large-scale dataset, the large evaluation networks contain 26 cells with initial channels of 56 and 50 for *ASRNET-C* and *ASRNET-D* respectively. Except for the model parameters, the maximum GPU memory is taken into account for different initial configurations. The networks are trained from scratch for 7 epochs with batch size 4. The large-sized CLDNN consists of 7 LSTM layers with 1536 nodes in each layer. As shown in Table 3, for the low latency setting, the network has achieved more than 19% (average on the four test sets) relative improvements compared with the CLDNN baseline. More than 11% relative improvements have been achieved by the network with the medium latency setting, compared with the low latency setting. Ablation study indicates that the CLDNN baseline with the low latency setting has obvious performance advantages over the very low latency setting. The training process takes around 7 days on 24 Tesla V100 GPUs.

4.5. Latency Computation

Some considerations in the latency computation are listed as follows: 1) The convolution with the kernel size 3×3 in the stem convolution layer produces extra 10ms latency. 2) The reduction cells share the searched architecture with the same algorithmic latency. 3) The latency of the second reduction cell is twice that of the first one for the operations with a stride of 2 at the beginning of the cell. As shown in the lower left of Figure 3, the path with the biggest receptive field contains the operations in sequence: *5x5 separable convolution, 5x1 then 1x5 convolution*. Based on the 60ms latency of the reduction cell, the total 190ms latency is induced for the low latency setting. As shown in the lower right of Figure 3, the path with the biggest receptive field includes: *5x5 separable convolution, 7x1 then 1x7 convolution, 7x1 then 1x7 convolution*. Considering the stacked sequential modules with a *ReLU-Conv-BN* order, the 180ms latency is computed for the reduction cell, so the total 550ms latency is induced for the medium latency setting.

5. Conclusions

In this paper, we focus on developing a streaming ASR model with NAS. We modify the macro architecture of NAS to restrict future context, and to search in the revised operation space to generate the architecture with low latency. We tested our method on a 10k-hour large-scale dataset. Experimental results demonstrated the great potential of our proposed approach. For the low latency setting, the searched model achieves 19% relative improvement compared with a CLDNN hybrid baseline model. Future work includes testing our method with transducer-based end-to-end streaming ASR systems.

6. References

- [1] J. Li, C. Liang, B. Zhang, Z. Wang, F. Xiang, and X. Chu, "Neural architecture search on acoustic scene classification," *arXiv preprint arXiv:1912.12825*, 2019.
- [2] S. Hu, X. Xie, S. Liu, M. Geng, X. Liu, and H. Meng, "Neural architecture search for speech recognition," *arXiv preprint arXiv:2007.08818*, 2020.
- [3] L. He, D. Su, and D. Yu, "Learned transferable architectures can surpass hand-designed architectures for large scale speech recognition," *arXiv preprint arXiv:2008.11589*, 2020.
- [4] Y.-C. Chen, J.-Y. Hsu, C.-K. Lee, and H.-y. Lee, "Darts-asr: Differentiable architecture search for multilingual speech recognition and adaptation," *arXiv preprint arXiv:2005.07029*, 2020.
- [5] B. Zhang, W. Li, Q. Li, W. Zhuang, X. Chu, and Y. Wang, "Autokws: Keyword spotting with differentiable architecture search," *arXiv preprint arXiv:2009.03658*, 2020.
- [6] S. Ding, T. Chen, X. Gong, W. Zha, and Z. Wang, "Autospeech: Neural architecture search for speaker recognition," *arXiv preprint arXiv:2005.03215*, 2020.
- [7] R. Luo, X. Tan, R. Wang, T. Qin, J. Li, S. Zhao, E. Chen, and T.-Y. Liu, "Lightspeech: Lightweight and fast text to speech with neural architecture search," *arXiv preprint arXiv:2102.04040*, 2021.
- [8] Y. Xu, L. Xie, X. Zhang, X. Chen, B. Shi, Q. Tian, and H. Xiong, "Latency-aware differentiable neural architecture search," *arXiv preprint arXiv:2001.06392*, 2020.
- [9] G. Li, M. Xu, S. Giancola, A. Thabet, and B. Ghanem, "Lc-nas: Latency constrained neural architecture search for point cloud networks," *arXiv preprint arXiv:2008.10309*, 2020.
- [10] M. Berman, L. Pishchulin, N. Xu, M. B. Blaschko, and G. Medioni, "Aows: Adaptive and optimal network width search with latency constraints," in *Proceedings of the IEEE/CVF Conference on Computer Vision and Pattern Recognition*, 2020, pp. 11 217–11 226.
- [11] J. Liu, S. Zhou, Y. Wu, K. Chen, W. Ouyang, and D. Xu, "Block proposal neural architecture search," *IEEE Transactions on Image Processing*, vol. 30, pp. 15–25, 2020.
- [12] B. Zoph, V. Vasudevan, J. Shlens, and Q. V. Le, "Learning transferable architectures for scalable image recognition," in *Proceedings of the IEEE conference on computer vision and pattern recognition*, 2018, pp. 8697–8710.
- [13] L. Xie, X. Chen, K. Bi, L. Wei, Y. Xu, Z. Chen, L. Wang, A. Xiao, J. Chang, X. Zhang *et al.*, "Weight-sharing neural architecture search: A battle to shrink the optimization gap," *arXiv preprint arXiv:2008.01475*, 2020.
- [14] H. Liu, K. Simonyan, and Y. Yang, "Darts: Differentiable architecture search," *arXiv preprint arXiv:1806.09055*, 2018.
- [15] X. Chen, L. Xie, J. Wu, and Q. Tian, "Progressive differentiable architecture search: Bridging the depth gap between search and evaluation," in *Proceedings of the IEEE International Conference on Computer Vision*, 2019, pp. 1294–1303.
- [16] A. v. d. Oord, S. Dieleman, H. Zen, K. Simonyan, O. Vinyals, A. Graves, N. Kalchbrenner, A. Senior, and K. Kavukcuoglu, "Wavenet: A generative model for raw audio," *arXiv preprint arXiv:1609.03499*, 2016.
- [17] A. Van Oord, N. Kalchbrenner, and K. Kavukcuoglu, "Pixel recurrent neural networks," in *International Conference on Machine Learning*. PMLR, 2016, pp. 1747–1756.
- [18] H. Bu, J. Du, X. Na, B. Wu, and H. Zheng, "Aishell-1: An open-source mandarin speech corpus and a speech recognition baseline," in *2017 20th Conference of the Oriental Chapter of the International Coordinating Committee on Speech Databases and Speech I/O Systems and Assessment (O-COCOSDA)*. IEEE, 2017, pp. 1–5.
- [19] J. Du, X. Na, X. Liu, and H. Bu, "Aishell-2: transforming mandarin asr research into industrial scale," *arXiv preprint arXiv:1808.10583*, 2018.
- [20] Z. You, D. Su, J. Chen, C. Weng, and D. Yu, "Dfsmn-san with persistent memory model for automatic speech recognition," in *ICASSP 2020-2020 IEEE International Conference on Acoustics, Speech and Signal Processing (ICASSP)*. IEEE, 2020, pp. 7704–7708.
- [21] T. Ko, V. Peddinti, D. Povey, and S. Khudanpur, "Audio augmentation for speech recognition," in *Sixteenth Annual Conference of the International Speech Communication Association*, 2015.
- [22] K. Chen and Q. Huo, "Scalable training of deep learning machines by incremental block training with intra-block parallel optimization and blockwise model-update filtering," in *ICASSP-2016*, March 2016.
- [23] T. N. Sainath, O. Vinyals, A. Senior, and H. Sak, "Convolutional, long short-term memory, fully connected deep neural networks," in *2015 IEEE international conference on acoustics, speech and signal processing (ICASSP)*. IEEE, 2015, pp. 4580–4584.
- [24] D. Amodei, S. Ananthanarayanan, R. Anubhai, J. Bai, E. Battenberg, C. Case, J. Casper, B. Catanzaro, Q. Cheng, G. Chen *et al.*, "Deep speech 2: End-to-end speech recognition in english and mandarin," in *International conference on machine learning*. PMLR, 2016, pp. 173–182.